Contents

Chapter 2

Executive Summary

2.1 Physics and overview

In the early 1970's, evidence that the masses of strongly interacting particles increased as their internal angular momentum increased led the Japanese theorist Yoichiro Nambu to propose that the quarks inside of these particles are tied together by strings [1]. The observed linear dependence of the square of the hadron masses on the spin of the hadrons comes about when the string has a constant mass per length.

Meanwhile, we have learned that the strong interactions are described by quantum chromodynamics (QCD), the field theory in which quarks interact through a *color* force carried by gluons. Numerical simulations of QCD – lattice QCD – have demonstrated that Nambu's conjecture was essentially correct: in chromodynamics, a string-like chromoelectric flux tube forms between distant static color charges, leading to quark confinement and a potential energy between a quark and the other quarks to which it is tied which increases linearly with the distance between them. This linear potential is equivalent to the constant mass per length of Nambu's strings. It qualitatively explains confinement – infinite energy would be needed to separate quarks to infinity. Confinement is the most novel and spectacular feature of QCD.

Figure 2.1 illustrates an estimate of the chromodynamic energy density in the vicinity of a quark and antiquark based on a lattice QCD calculation [2]. The energy peaks at the positions of the quarks and in the space between the quarks the energy is confined to a flux tube. Such flux tubes arise because of the self-interaction of the gluons of QCD. In contrast the photons of QED do not carry electrical charge and thus do not form flux-tubes. The electric field lines between electric charges fill all space.

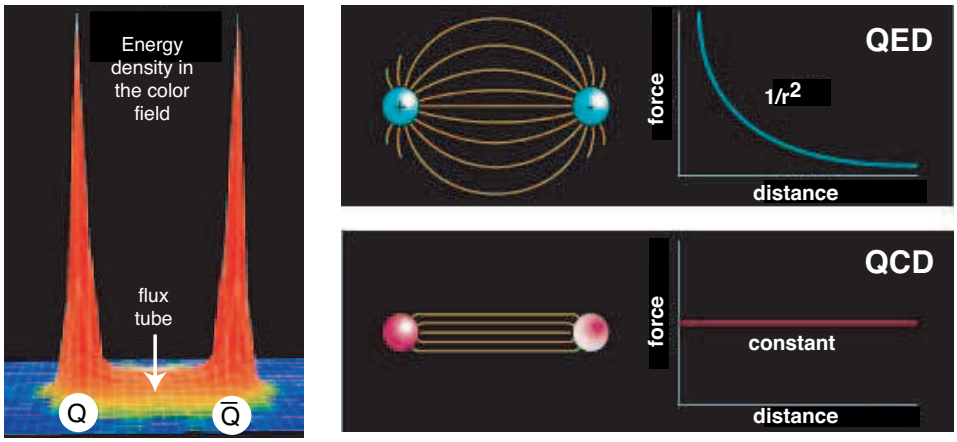

Figure 2.1: (left) A lattice QCD calculation of the energy density in the color field between a quark and an anti-quark. The density peaks at the positions of the quarks and is confined to a tube between the quarks. This calculation is for heavy quarks in the quenched approximation. (right) Field lines associated with the electrical force between two electrically charged particles (top) and the corresponding dependence of force on the distance between the charges and the field lines associated with the color force (bottom) between two quarks and the corresponding dependence of force on distance.

The ideal experimental test of this new feature of QCD would be to directly study the flux tube of Figure 2.1 directly by anchoring a quark and antiquark several femtometers apart and examining the flux tube that forms between them. In such ideal circumstance, one of the fingerprints of the gluonic flux tube would be the model-independent spectrum characterized by the two degenerate first excited states, which are the two longest wavelength vibrational modes of this system. Their excitation energy is π/r (r is the separation between the quarks) since both the mass and the tension of this relativistic string arise from the energy stored in its color force fields.

Such a direct examination of the flux tube is of course not possible. In real life we have to be content with systems in which the quarks move. Fortunately, we know both from general principles and from lattice QCD that an approximation to the dynamics of the full system which ignores the impact of these two forms of motion on each other works quite well - at least down to the charm quark mass.

To extend the flux tube picture to yet lighter quarks models are required, but the most important properties of this system are determined by the model-independent features described above. In particular, in a region around 2 GeV/c^2,

a new form of hadronic matter must exist in which the gluonic degree of freedom of mesons is excited. The unique characteristic of these new states is that the vibrational quantum numbers of the string, when added to those of the quarks, can produce a total angular momentum J, a total parity P, and a total charge conjugation symmetry C not allowed for ordinary $q\bar{q}$ states. These unusual J^{PC} combinations, like 0^{+-}, 1^{-+}, and 2^{+-}, are called exotic, and the states are referred to as exotic hybrid mesons.

Not only general considerations and flux tube models, but also first-principles lattice QCD calculations, require that these states be in this 2 GeV/c^2 mass region, while also demonstrating that the levels and their orderings will provide experimental information on the mechanism which produces the flux tube. Moreover, tantalizing experimental evidence has appeared over the past several years for exotic hybrids as well as for gluonic excitations with no quarks (glueballs).

Photon beams are expected to be particularly favorable for the production of the exotic hybrids. The reason is that the photon sometimes behaves as a virtual vector meson (a $q\bar{q}$ state with the quark spins parallel, adding up to total quark spin $S = 1$). When the flux tube in this $q\bar{q}$ system is excited to the first excited levels, both ordinary and exotic J^{PC} are possible. In contrast, when the spins are antiparallel ($S = 0$), as in pion or kaon probes, the exotic combinations are not generated. Thus photons are expected to produce exotics more directly than other meson probes. To date, most meson spectroscopy has been done with incident pion or kaon probes. High flux photon beams of sufficient quality and energy have not been available, so there are virtually no data on the photoproduction of mesons below 3 GeV/c^2. Thus, experimenters have not been able to search for exotic hybrids precisely where they are expected to be found.

The GlueX detector is optimized for incident photons in the energy range from 8 to 9 GeV in order to access the desired meson mass range. The use of a solenoidal spectrometer allows for the measurement of charged particles with excellent efficiency and momentum determination. At the same time, the solenoidal field acts as a magnetic shield, containing the shower of unwanted electron-positron pairs associated with the photon beam. Photons will be produced using the coherent bremsstrahlung technique by passing an electron beam from the CEBAF accelerator though a wafer-thin diamond crystal. At special settings for the orientation of the crystal the atoms of the crystal can be made to recoil together from the radiating electron leading to an enhanced emission at particular photon energies and yielding linearly polarized photons.

Even with only 10% of the eventual photon fluxes of 10^8/sec from the continuous CEBAF beam, the experiment will accumulate statistics during

the first year of operation which will exceed extant published data with pions by at least an order of magnitude. With the GLUEX detector, high statistics, and the linear polarization information, it will be possible to map out the full spectrum of these gluonic excitations.

In order to achieve the required photon energy and flux with coherent bremsstrahlung, an electron beam of 12 GeV is required. Figure 2.2 shows the current accelerator complex with the existing three experimental Halls A, B and C and the planned HALL D. The addition of state-of-the-art accelerating units (*cryomodules*) in the existing space in the linear sections of the accelerator, along with upgrading of magnets in the arcs, will bring the electron energy up from the current maximum of 5.5 GeV to 12 GeV.

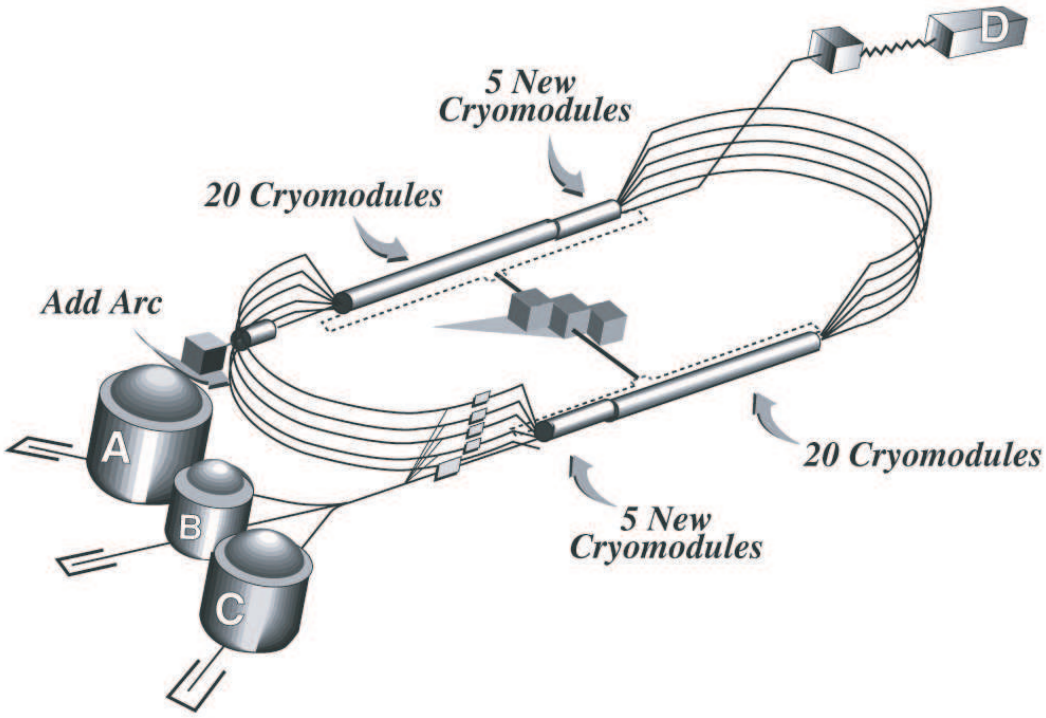

Figure 2.2: The current CEBAF multi-pass electron accelerator at JLab, showing the three existing experimental Halls (A, B and C) and the planned Hall D.

When the spectrum and decay modes of these gluonic excitations have been mapped out experimentally, we will have made a giant step forward in understanding the confinement mechanism in QCD.

In this Design Report we expand on:

1. *Spectroscopy of Light Mesons.* This will include a brief review of the conventional quark model and the status of the light quark meson spectrum.

2. *Gluonic excitations and their role in QCD.* This will include a discussion of how the gluons form flux tubes, and how their excitations lead to QCD mesons, in particular exotic hybrids. This general picture is not restricted to a particular model but follows from the first-principles QCD calculations.

3. *The current evidence for gluonic excitations.* The evidence comes from overpopulation of conventional nonets and from possible glueball and exotic hybrid sightings in $\bar{p}p$ annihilations and π-induced interactions.

4. *Photons are expected to be particularly effective in producing exotic hybrids.* Its spin structure makes the photon a qualitatively different probe from π and K beams. The first excited transverse modes of the flux tube can lead to exotic hybrids only when the quark spins are aligned. This argument is consistent with expectations from models based on phenomenological analysis of existing data that predict cross sections for photoproduction of exotic hybrids comparable to those of normal mesons. And there are essentially no data on photoproduction of light mesons so this is *Terra incognito.* The existing photoproduction data will be discussed.

5. *The complementarity of this study with other planned projects that will study gluonic excitations.* We will compare this to searches in the charm quark or beauty quark sectors or e^+e^- annihilations, in particular the GSI Project and the CLEO-c Project at Cornell.

6. *The importance of the PWA technique in uncovering exotic mesons.* The PWA is a powerful analysis tool that has been successfully employed in experiments to uncover states which are not evident from a simple examination of mass spectra (bump-hunting). PWA is absolutely essential for this project as is the development of the formalism for incident photon beams and an understanding of the phenomenology. The importance of a hermetic detector with excellent resolution and rate capability and sensitivity to a wide variety of decay modes will be discussed.

7. *Linear polarization of the photon beam is essential for this study.* Linear polarization is important in the determination of the J^{PC} quantum numbers and it is essential in determining the production mechanism.

Linear polarization can be used as a filter for exotics once the production mechanism is isolated.

8. *The ideal photon energy range.* In order to reach the desired mass range we need to be far enough above threshold so that the decay products of produced mesons can be detected and measured with sufficient precision. Sufficient energies are also required to avoid line-shape distortions of higher-mass mesons. We also want to be high enough in energy to kinematically separate production of baryon resonances from production of meson resonances. This need for higher energies, however is balanced by a need for sufficiently low energy to allow for a solenoid-only-based detector to momentum analyze the highest energy charged particles with sufficient accuracy. These considerations lead to an ideal photon energy in the range from 8 to 9 GeV.

9. *The desired electron energy.* Having established the desired photon beam beam energy of 9 GeV an electron energy must be sufficiently high compared to the desired photon beam energy to achieve a sufficient degree of linear polarization. With 12 GeV electrons, the degree of linear polarization is 40%. If the electron energy drops to 10 GeV the degree of polarization drops to 5%. The ratio of tagged hadronic rate to total hadronic rate in the detector drops as the electron energy approaches the desired photon energy. The conclusion is that an electron energy of 12 GeV suffices but lower energies will severally compromise the physics goals.

The optimal choice for the photon energy drives the electron energy needed for this study.

2.2 Photon beam and choice of energy

What is the optimal photon beam energy to carry out the GlueX physics goals? The goal of this experiment is to search for mesons in the mass range up to 2.5 GeV/c^2 in the reaction $\gamma p \to Xp$, as shown in Figure 2.3. The minimum beam photon energy to produce a particle of mass m_X in the reaction $\gamma p \to Xp$ is given by equation 2.1. An incident photon energy of 5.8 GeV is sufficient to produce a meson of mass 2.5 GeV/c^2. However, it is necessary to operate above this energy to produce mesons with adequate yield and boost so that the decay products can be detected and measured with sufficient precision.

$$E_\gamma = m_X \cdot \left(1 + \frac{m_x}{2m_p}\right) \tag{2.1}$$

The momentum-transfer-squared (t) between the incident photon (γ) and the produced meson (X) in the reaction $\gamma p \to Xp$ is given by:

$$t = (p_\gamma - p_X)^2 \tag{2.2}$$

and at incident photon energies of several GeV and above, the distribution in t is given by:

$$dN/dt = e^{\alpha t} \tag{2.3}$$

The yield is determined by the value of the minimum value of the momentum-

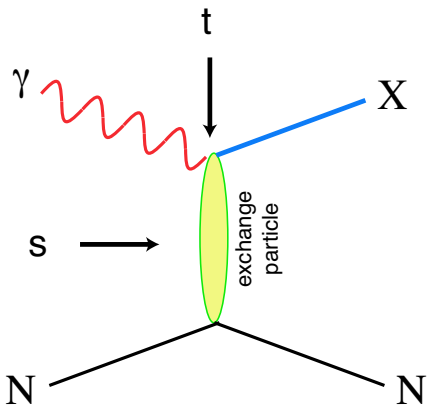

Figure 2.3: Diagram for the photoproduction of particle X. The variables s and t are the center-of-mass energy squared and the momentum-transfer-squared from incoming photon to outgoing particle X. The process shown here proceeds through the exchange of a particle in the t-channel.

transfer-squared from incoming beam to outgoing particle X, $|t|_{min}$, and the exponential falling distribution in $|t|$. For a given photon beam energy, E_γ, $|t|_{min}$ depends on m_X – increasing with increasing m_X for fixed E_γ and decreasing with increasing E_γ for fixed m_X. The variation of $|t|_{min}$ with m_X is rapid for m_X near the kinematic limit leading to a severe damping of the yield of mesons and a distortion of the line shape since the variation of $|t|_{min}$ over the Breit-Wigner width of a resonance can be significant.

Another consideration is the ability to kinematically separate meson resonance production from baryon resonance production. As an example, we

considered various reactions leading to a final state: $\pi^+\pi^-\pi^+n$. We enumerate the possibilities:

$$\gamma p \to X^+ n \to \rho^0\pi^+ n \to \pi^+\pi^-\pi^+ n \tag{2.4}$$

$$\gamma p \to \rho^0\Delta^+ \to \rho^0\pi^+ n \to \pi^+\pi^-\pi^+ n \tag{2.5}$$

$$\gamma p \to \pi^+ N^{*0} \to \pi^+\pi^-\pi^+ n \tag{2.6}$$

Suppose that the first of these is the reaction of interest. We can reduce effects from the other two by requiring that the effective mass of any πn or $\pi\pi n$ combination be outside the baryon resonance region. In this exercise we define the baryon region to include πn or $\pi\pi n$ mass combinations below 1.7 GeV/c^2. The fraction of events for which we are able to reduce the offending reactions, as a function of beam momentum and for various m_X masses is a factor in estimating the overall figure-of-merit.

Whereas the considerations mentioned thus far favor larger photon beam energies, other considerations favor a lower photon beam energy. For a given electron energy, the flux of photons and the degree of linear polarization of the photon beam will decrease rapidly as the energy of the photons approaches that of the electrons.

The partial wave analysis (PWA) technique will be used to extract information about the spin and parity of produced states. With a photon beam this process is greatly aided by using photons that are linearly polarized. Linear polarization is essential to correlate characteristics of the exchange mechanism with that of the produced meson. Linear polarization can be achieved by using Compton backscattering or coherent bremsstrahlung off a crystal. The electron energies required and other practical technical limitations involving mirrors and lasers preclude the former for the photon fluxes and energies required. The latter option will be employed and is possible because the stringent requirements placed on the electron beam are realizable with the CEBAF accelerator. The details of how the tagged and collimated coherent beam will be produced are discussed in Chapter 4 of this Design Report.

For the tagged and collimated coherent photon beam the variation in flux, for constant total hadronic rate in the detector, is plotted in Figure 2.4 as a function of photon beam energy for three different values of electron energy. In Figure 2.4 the degree of linear polarization is plotted as a function of photon beam energy for three different values for the electron energy as well.

In Figure 2.5 we plot an overall figure-of-merit which folds in the variation of beam flux and degree of linear polarization with beam energy, as well as

the effective yield taking into account $|t|_{min}$ effects and the ability to separate meson resonances from baryon resonances kinematically.

Finally, we note that with a solenoid-only-based detector the maximum photon beam energy is again about 9 GeV. Above that energy, charged products from two-body decays of produced resonances – especially of lower mass – will not be momentum-analyzed with sufficient precision. The solenoid-only geometry is essential for this high-flux photon beam to contain the electromagnetic backgrounds, e.g. e^+e^- pairs, within the beam pipe – the axial field will result in helical trajectories for the electromagnetically produced charged background.

From all this we conclude that the optimum photon beam energy is between 8 and 9 GeV. For this photon energy the maximum electron energy achievable within the confines of the the current CEBAF, 12 GeV, is adequate in terms of flux and degree of linear polarization. However the degree of linear polarization at 9 GeV falls rapidly – from 40% at $E_e = 12$ GeV to 5% at $E_e = 10$ GeV.

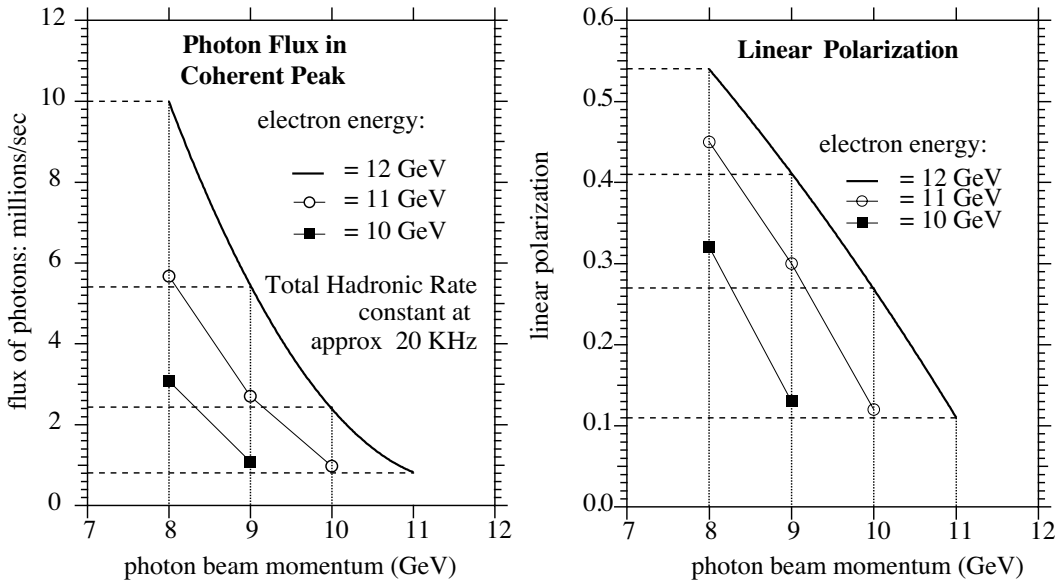

Figure 2.4: (left) The flux of photons in the coherent peak for a constant total hadronic rate in the detector of $\approx$ 20 KHz as a function of beam photon energy. (right) The degree of linear polarization of photons in the coherent peak as a function of beam energy. In both cases the electron energy is 12 GeV.

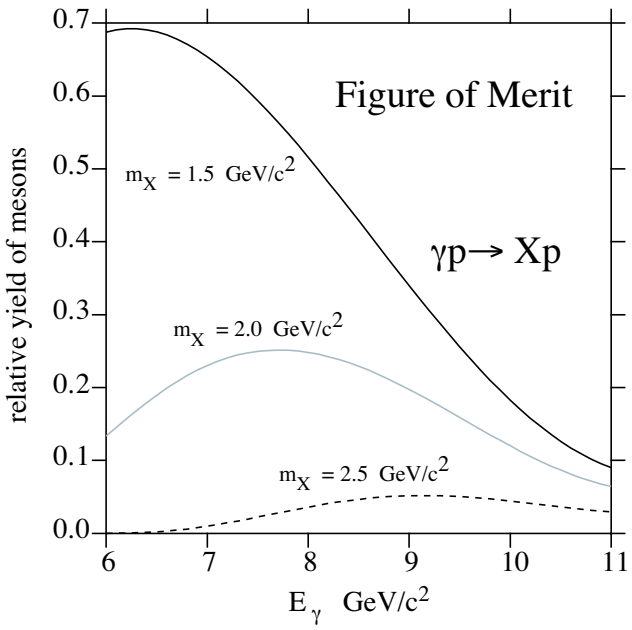

Figure 2.5: An estimate of the overall figure of merit for producing mesons as a function of photon beam energy for three different meson masses.

2.3 Detector and solenoid

The physics goals of the GlueX project require a full PWA of kinematically identified exclusive reactions producing mesons. The decay products of produced mesons must be identified and measured with good resolution and with full acceptance in decay angles. In many cases, the decays of mesons involve a chain of particle decays. The GlueX detector must therefore be hermetic with 4π coverage with the capability of measuring energies of neutral particles (γ, π^0, η) and momenta of charged particles with good resolution. Particle identification is also required.

Figure 2.6 shows a schematic of the GlueX detector. It is based on solenoid-only detector design – optimal for dealing with the electromagnetic backgrounds produced in the target with the high-flux photon beam. The superconducting solenoidal magnet is the LASS/MEGA magnet. This magnet was built for the Large Aperture Superconducting Solenoid Spectrometer (LASS) at SLAC and later transferred to LANL for use in the MEGA experiment. As assessment team consisting of the originally magnet designers and users, GlueX personnel and LANL MEGA users visited LANL to review the magnet status. The magnet is in fine shape and will be moved to the Indiana

University Cyclotron Facility (IUCF) for refurbishment. The move is scheduled for November, 2002. More details about the magnet are given in Chapter 5.

The GLUEX detector described in Chapter 6 is optimized for photon beam energies between 8 and 9 GeV. The detector consists of a large aperture superconducting solenoid filled with a target, tracking chambers and calorimetry. The calorimetry will also provide time-of-flight information for particle identification. The solenoid will be followed with a threshold Čerenkov counter, particle tracking, a forward TOF and a lead glass electromagnetic calorimeter. The forward electromagnetic calorimeter will be a modified version of the lead glass detector used in Brookhaven experiment E852. That detector has already been moved to JLab.

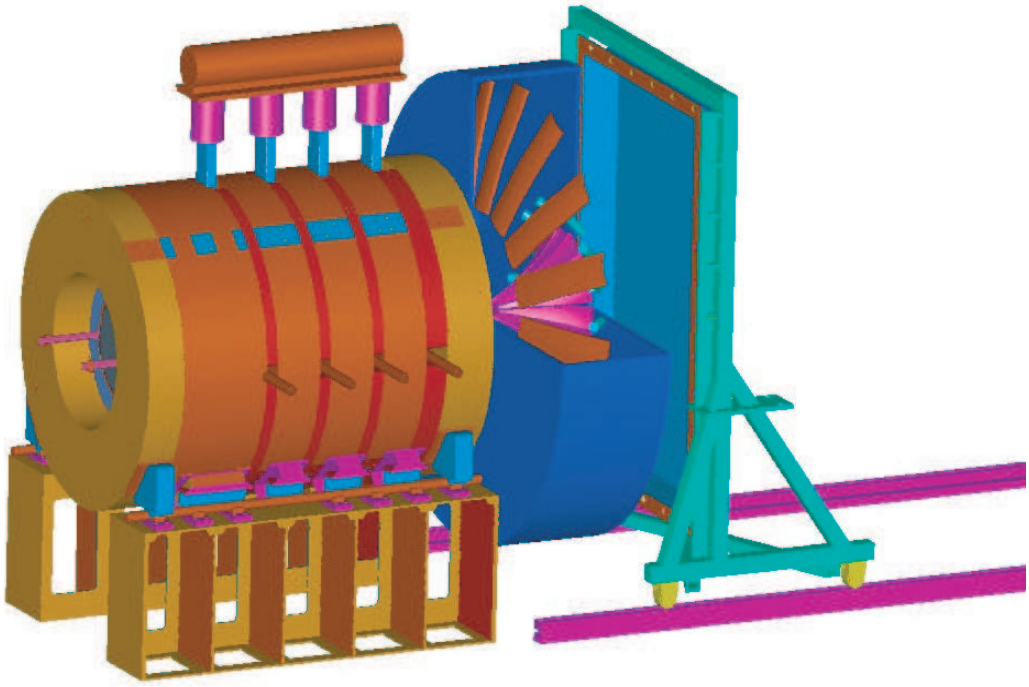

Figure 2.6: The detector for the GLUEX experiment.

2.4 Electronics

The goal of the GLUEX readout electronics system is to digitize and read out the detector signals for level 1 trigger rates of up to 200 kHz without incurring

dead time. A pipelined approach is required. The digitized information will be stored for several μs while the level 1 trigger is formed. Multiple events must be buffered within the digitizer modules and read while the front ends continue to acquire new events.

Two basic types of readout electronics will be used in GLUEX, FADCs and TDCs. Detectors which measure energy will be continuously sampled with flash ADCs while detectors which require precise time measurements will use a multi-hit TDC. No currently available commercial solutions exist. These boards will be designed by our collaboration. Prototypes have been constructed, and are being tested.

The number of channels in the GLUEX detector is not large enough to justify the financially risky development of custom integrated circuits. Programmable logic devices are fast enough and available at reasonable cost. Programmable logic also allows for optimization of the data path without redesigning a printed circuit. ICs developed for other experiments will also be used.

Electronics technology is constantly evolving, and the optimum solution for the GLUEX detector depends on when funding becomes available and the construction schedule. A preliminary design that could be implemented with currently available components is presented in Chapter 7.

2.5 Rates and triggers

The GLUEX experiment will begin data taking with an event rate of $\approx 10^7$ tagged γ/s. Using only the hardware, (level 1) trigger, the total rate to tape will be approximately 15,000 events per second, (both interesting physics and backgrounds). As the tagged photon flux is raised toward its ultimate design goal of $10^8\,\gamma/s$, a software (level 3) trigger will be implemented to maintain the $15\,kHz$ rate to tape. Details about the trigger design and further discussions about rates and backgrounds are given in Chapter 8.

2.6 Computing

GLUEX will be the first Jefferson Laboratory experiment to generate petabyte scale data sets on an annual basis (One petabyte= 1 $PB = 10^{15}$ Bytes). In addition, generating physics results in a timely fashion has been identified as a primary goal of our collaboration since its inception. For these reasons, a well-designed, modern, and efficient computing environment will clearly be crucial to the success of the experiment.

Currently, there are a number of particle physics projects world wide which also will produce very large data sets, and which will function with large dispersed collaborations. It seems quite reasonable, then, to expect that over the coming years, many new tools will be developed which will aid in effectively processing and managing these large volumes of data. As a collaboration, we will undoubtedly make effective use of these tools, which will include such things as grid middle ware, distributed file systems, database management tools, visualization software, and collaborative tools.

Nonetheless, it also is clear that the GlueX collaboration will need to develop a suite of tools which are dedicated to this experiment. This will include data acquisition and trigger software, experiment monitoring and control software, data reduction tools, physics analysis software, and tools dedicated to the partial wave analysis (PWA) effort. The plan is described in Chapter 9.

2.7 Monte Carlo

Monte Carlo simulations of photoproduction reactions and the detector response are an integral part of data analysis for GlueX. Monte Carlo data sets, which are an order of magnitude larger than the real data for specific channels, must be produced and analyzed within a unified analysis framework. The computer resources needed for this task are discussed in Chapter 9. Chapter 10 describes how the simulation is to be carried out, the specific software components that exist at present, and some preliminary results regarding detector acceptance and resolution.

2.8 PWA

To identify the J^{PC} quantum numbers of a meson it is necessary to perform a *partial wave analysis* (PWA). In the simplest terms, a partial wave analysis determines production amplitudes by fitting decay angular distributions. The fit includes information on the polarization of the beam and target, the spin and parity of the resonance, the spin and parity of any daughter resonances and any relative orbital angular momenta. The analysis seeks to establish the production strengths, production mechanisms and the relative phase motion of various production amplitudes. Phase motion is critical in determining if resonance production is present.

Although the methodology is in principle straightforward, there are issues that complicate the implementation. Mathematical ambiguities must be dealt

with. Issues of where to truncate the series expansion are important. And the theoretical underpinnings, including issues of analyticity, unitarity and S-matrix theory need to addressed. Chapter 11 discusses both results of detailed PWA analysis carried out to date, and the plans for carrying out the PWA in the experiment.

2.9 Cassel review

A review of the GlueX/Hall D Project by a committee chaired by David Cassel of Cornell was held in late 1999. The committee, consisting of high energy and nuclear experimentalists and theorists, issued its report in early 2000. The conclusion was that GlueX is poised to do the definitive search for exotic hybrids and that JLab is unique for this search. Their report is included in Appendix A.

2.10 Management plan

The GlueX collaboration has adopted a management plan based on the experience of other collaborations at JLab and collaborations in high energy physics. This plan is described in Appendix B.

2.11 NSAC report

In Spring of 2002, the Nuclear Science Advisory Committee (NSAC) released its long-range plan for nuclear physics. One of the four recommendations of this plan is to quickly carry out the 12 GeV CEBAF Upgrade and the physics program of GlueX. Appendix C summarizes those parts of the long-range plan that are relevant the the upgrade.

2.12 Civil construction

The plan is to site the meson spectrometer in a new experimental hall (Hall D) to be located at the end of a new beam line which would come off the stub at the east end of the north linac of CEBAF. The civil construction includes work associated with breaking through the stub, delivering beam above ground to a tagging spectrometer, a tagger building, Hall D, the counting house, roads, and a parking area. Members of the GlueX collaboration have been meeting

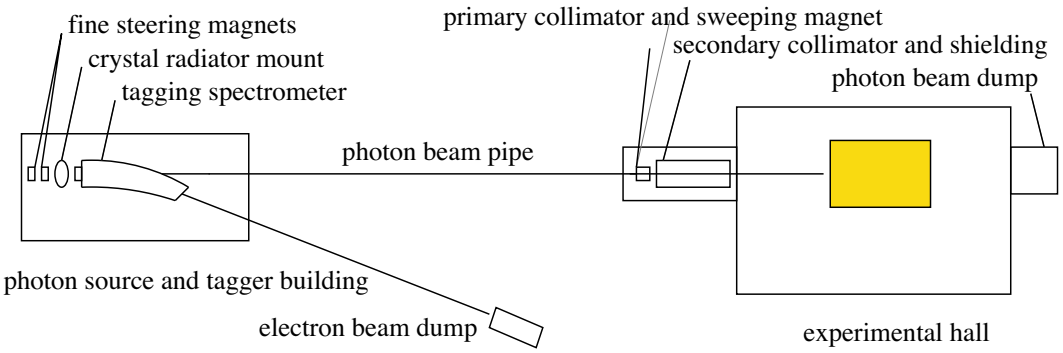

Figure 2.7: Schematic showing the photon beam line into HALL D housing the GLUEX experiment.

with members the JLab civil construction team to arrive at a cost estimate and milestones for civil construction. Figure 2.7 shows a schematic of the beam delivery system and HALL D. Details are given in Appendix D.

List of Figures

List of Tables

Bibliography

[1] Y. Nambu. Univ. of Chicago report No. 70-70, 1970.

[2] G. Bali *et al.* (SESAM Collaboration). Static potentials and glueball masses from QCD simulations with Wilson loops. *Phys. Rev.*, D**62**:054503, 2000. hep-lat/0003012.